

Strange hadron(K_S^0 , Λ and Ξ) elliptic flow from 200 GeV
 $Cu + Cu$ collisions

Shusu Shi for the STAR collaboration

¹ Nuclear Science Division, LBNL, Berkeley 94720, USA

² Institute of Particle Physics, CCNU, Wuhan 430079, China

Abstract. Collective flow reflects dynamical evolution in high-energy heavy ion collisions. In particular, the strange hadron elliptic flow reflects early collision dynamics [1]. We present results from a systematic analysis of the centrality dependence of strange hadron elliptic flow (v_2) measurement of K_S^0 , Λ and Ξ for $Cu + Cu$ collisions at 200 GeV. Results for $Cu + Cu$ collisions are compared with results previously reported for $Au + Au$ collisions. We will also compare our data with results from ideal hydrodynamic calculations.

Keywords: heavy ion collisions, elliptic flow, hydrodynamic model

PACS: 25.75.Ld, 25.75.Dw

1. Introduction

The characterization of the elliptic flow of produced particles by their azimuthal anisotropy has been proven to be one of the most fruitful probes of the dynamics in $Au + Au$ collisions at the Relativistic Heavy Ion Collider(RHIC) [3, 4, 5, 6, 7]. Study elliptic flow in smaller collision systems, such as $Cu + Cu$, which has one-third nucleons in $Au + Au$, is beneficial. Because exactly how flow scales with collision systems, such as system size, geometry, constituent quarks, transverse momentum and transverse energy, is crucial to the understanding of the properties of the produced matter. Hydrodynamic model calculations, with the assumption of ideal fluid behavior (no viscosity), have been successful when compared with the experimental data at RHIC [10, 11]. In this proceeding, we extend the comparison with ideal hydrodynamic calculations to different systems.

2. Methods and Analysis

In this proceeding, we report results from $\sqrt{s_{NN}} = 200$ GeV $Cu + Cu$ collisions. Data were taken from Run 5 (2005). STAR's Time Projection Chamber (TPC) [14] is used as the main detector for particle identifications. The centrality was deter-

	<i>Cu + Cu</i>			<i>Au + Au</i>
	0-60%	0-20%	20-60%	0-80%
$dN_{ch}/d\eta$	74	132	45	225
N_{part}	51	87	34	126
N_{bin}	80	156	43	293
ε_{part}	0.252	0.184	0.393	0.214

Table 1. List of $dN_{ch}/d\eta$, number of participants N_{part} , number of binary collisions N_{bin} , and participant eccentricity ε_{part} for three centrality bins in 200 GeV *Cu + Cu* collisions and 0-80% 200 GeV *Au + Au* collisions.

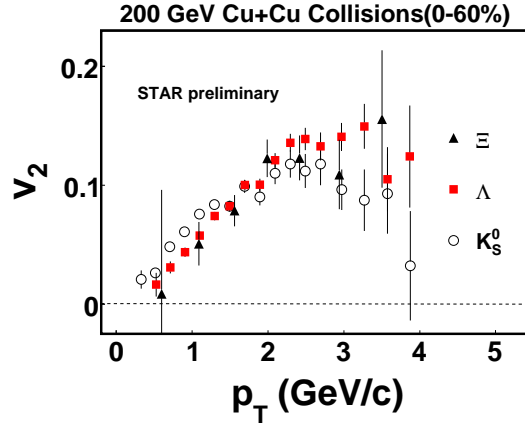


Fig. 1. v_2 as a function of p_T for K_S^0 (open-circles), Λ (filled-squares) and Ξ (filled-triangles) in 0-60% *Cu + Cu* collisions at $\sqrt{s_{NN}} = 200$ GeV.

mined by the number of tracks from the $|\eta| \leq 0.5$. Two Forward Time Projection Chambers (FTPCs) were also used for event plane determinations. FTPC has the coverage of $2.5 \leq |\eta| \leq 4$, and the pseudorapidity between FTPC and TPC allows us to reduce some of the non-flow effects.

The PID is achieved via topologically reconstructed hadrons: $K_S^0 \rightarrow \pi^+ + \pi^-$, $\Lambda \rightarrow p + \pi^-$ ($\bar{\Lambda} \rightarrow \bar{p} + \pi^+$) and $\Xi^- \rightarrow \Lambda + \pi^-$ ($\Xi^+ \rightarrow \bar{\Lambda} + \pi^+$). The detailed description of the procedure can be found in Refs. [8, 9].

v_2 analysis was done in three centrality bins. The corresponding number of charged hadrons, number of participants, number of binary collisions, and the participant eccentricity for each centrality bin are listed in Table I. For comparison, parameters for 0-80% *Au + Au* collisions are also listed in the table.

The observed v_2 is the second harmonic of the azimuthal distribution of particles with respect to this event plane:

$$v_2^{obs} = \langle \cos[2(\phi - \Psi_2)] \rangle \quad (1)$$

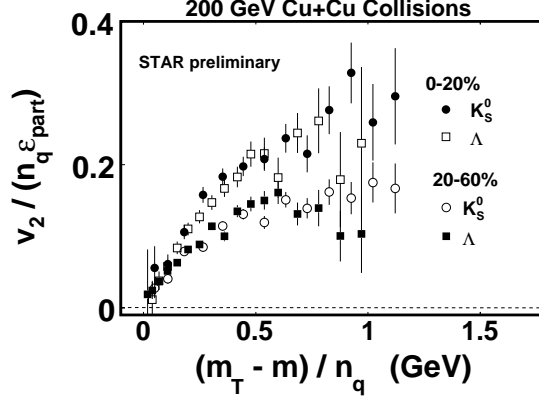


Fig. 2. The eccentricity (ϵ_{part}) and number of quark (n_q) scaled v_2 versus $(m_T - m)/n_q$ from 0-20% (filled-circles: K_S^0 , open-squares: Λ) and 20-60% (open-circles:

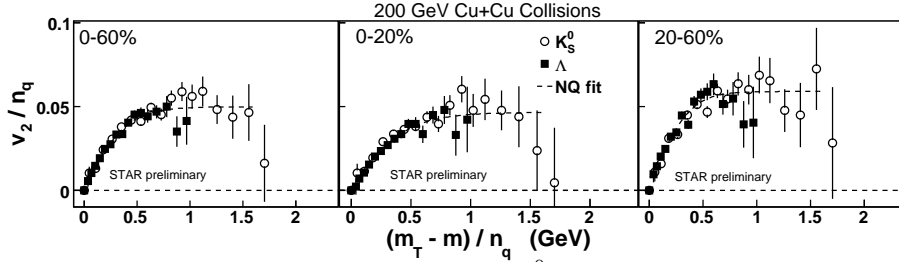


Fig. 3. Number of quark (n_q) scaled v_2 for K_S^0 (open-circles) and Λ (filled-squares) as a function of $(m_T - m)/n_q$ from three centrality bins. The results of the fits [13] are shown as dashed-lines in the figure.

where angle brackets denote an average over all particles with their azimuthal angle ϕ in a given phase space. To take into account the smearing of the estimate event plane around the true reaction plane, the real v_2 has to be corrected for the event plane resolution by

$$v_2 = \frac{v_2^{obs}}{\langle \cos[2(\Psi_2 - \Psi_r)] \rangle} \quad (2)$$

For v_2 of the identified particles, K_S^0 , Λ and Ξ , the v_2 versus m_{inv} method [12] is used in this analysis. We use Λ (Ξ) to denote $\Lambda + \bar{\Lambda}$ ($\Xi^- + \bar{\Xi}^+$) unless stated otherwise.

3. Results

Figure 1 shows v_2 as a function of p_T for K_S^0 (open-circles), Λ (filled-squares) and Ξ (filled-triangles) in 0-60% $Cu + Cu$ collisions at $\sqrt{s_{NN}} = 200$ GeV. At low p_T , Λ

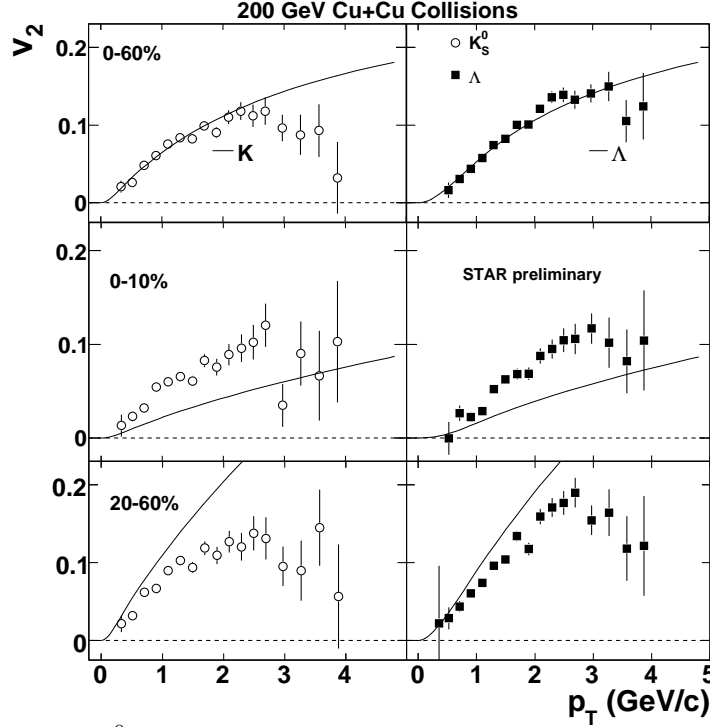


Fig. 4. v_2 of K_S^0 (open-circles) and Λ (solid-squares) as a function of p_T for three centralities 0-60%, 0-10% and 20-60% in $Cu + Cu$ collisions at $\sqrt{s_{NN}} = 200$ GeV. For comparison, ideal hydrodynamic calculations are also shown as lines.

v_2 is smaller than K_S^0 ; At high p_T , baryon(Λ , Ξ) v_2 is systematically greater than meson(K_S^0). K_S^0 and Λ v_2 cross over at p_T 1.5 - 2.0 GeV.

Figure 2 shows n_q -scaled v_2 normalized by participant eccentricity as a function of $(m_T - m)/n_q$ for K_S^0 and Λ from 0-20% and 20-60% $Cu + Cu$ collisions at $\sqrt{s_{NN}} = 200$ GeV. The participant eccentricity ε_{part} are from a Monte Carlo Glauber calculation. (See Table 1 for ε_{part} .) After the geometric effect has been removed by dividing by ε_{part} , the build-up of stronger collective motion in more central collisions becomes obvious in the measured elliptic flow.

Number of quark scaling was observed in 200 GeV $Au + Au$ collisions firstly. In Figure 3, we test n_q scaling in 200 GeV $Cu + Cu$ collisions. At low and intermediate p_T , scaling works well; At high p_T , v_2 for K_S^0 and Λ have large error bars, but are consistent with n_q fitted curve. We can draw the conclusion: Number-of-Quark scaling was also observed in 200 GeV $Cu + Cu$ collisions.

Hydrodynamic model can be used to calculate elliptic flow in heavy ion collisions, preliminary ideal hydrodynamic model results are from Pasi Huovinen. In

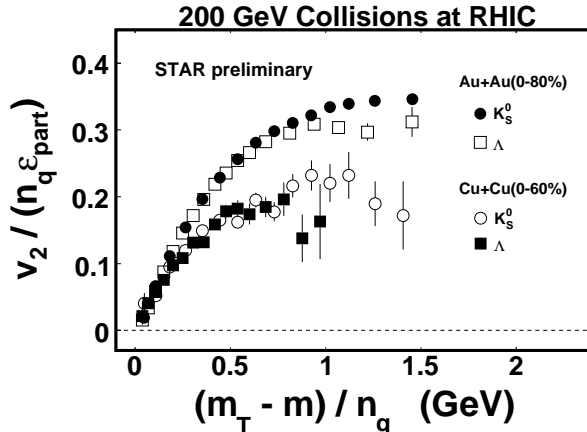


Fig. 5. The eccentricity (ε_{part}) and number of quark (n_q) scaled v_2 versus $(m_T - m)/n_q$ from 0-60% $Cu + Cu$ (open-circles: K_S^0 , filled-squares: Λ) and 0-80% $Au + Au$ collisions (filled-circles: K_S^0 , open-squares: Λ) at $\sqrt{s_{NN}} = 200$ GeV.

Figure 4, we compare experimental data to ideal hydrodynamic model results in different centrality bins. In central collisions, ideal hydrodynamic model under-predicts v_2 ; in peripheral collisions, ideal hydrodynamic model over-predicts v_2 .

In order to study the system size dependence of scaling behavior, we normalize the n_q -scaled elliptic flow (v_2) by the participant for different systems. (See Table 1 for ε_{part} .) Figure 5 shows the doubly scaled quantities from 200 GeV 0-60% $Cu + Cu$ and 0-80% $Au + Au$ collisions. After the geometric effect has been removed by dividing by ε_{part} , the build up of stronger collective motion in larger system becomes obvious, which is similar to the centrality dependence in $Cu + Cu$ and $Au + Au$ collisions [15] at $\sqrt{s_{NN}} = 200$ GeV. If hydrodynamic limit has been reached, v_2/ε_{part} should be a constant for $Cu + Cu$ and $Au + Au$ collisions [16]. This indicates that hydrodynamic limit has not been saturated in $Cu + Cu$ collisions.

4. Summary

We present STAR preliminary results of v_2 for K_S^0 , Λ and Ξ from 200 GeV $Cu + Cu$ collisions at RHIC. In order to reduce non-flow effects, FTPC tracks have been used to estimate the event plane. At low p_T , v_2 is found to be consistent with mass ordering. Number-of-Quark scaling was also observed in 200 GeV $Cu + Cu$ collisions at three centrality bins. Preliminary ideal Hydrodynamic model results are used to compare with experimental data. It under-predicts the elliptic flow in central collisions, over-predicts the elliptic flow in peripheral collisions. Stronger collective flow can be observed in the more central collisions or the larger system. v_2/ε_{part} is not a constant for $Cu + Cu$ and $Au + Au$ collisions. This indicates that

hydrodynamic limit has not been saturated in $Cu + Cu$ collisions.

5. Acknowledgments

Many thanks to the organizers; many thanks to P. Huovinen for discussions. The author is supported in part by NSFC under project 10775058 and MOE of China under project IRT0624.

References

1. J. Adams, et al., (STAR Collaboration), Nucl. Phys. **A757**, 102 (2005).
2. B.I. Abelev, et al., (STAR Collaboration), Phys. Rev. Lett., **99**, 112301(2007).
3. J. Adams et al., (STAR Collaboration), Phys. Rev. Lett. **93**, 252301 (2004).
4. J. Adams et al., (STAR Collaboration), Phys. Rev. **C 72**, 014904 (2005).
5. B.B. Back et al., (PHOBOS Collaboration), Phys. Rev. **C 72**, 051901 (2005).
6. B.B. Back et al., (PHOBOS Collaboration), Phys. Rev. Lett. **94**, 122303 (2005).
7. S.S. Adler et al., (PHENIX Collaboration), Phys. Rev. Lett. **94**, 232302 (2005).
8. C. Adler *et al.* (STAR Collaboration), Phys. Rev. Lett. **89**, 132301 (2002).
9. J. Adams *et al.* (STAR Collaboration), Phys. Rev. Lett. **92**, 052302 (2004).
10. J. Adams *et al.* (STAR Collaboration), Phys. Rev. C **72**, 014904 (2005).
11. J. Adams *et al.* (STAR Collaboration), Nucl. Phys. **A757**, 102 (2005).
12. N. Borghini, J.-Y. Ollitrault, Phys. Rev. C **70**, 064905 (2004).
13. X. Dong et al. Phy. Lett. **B597**, (2004)328
14. K. H. Ackermann *et al.* (STAR Collaboration), Nucl. Instrum. Methods A **499**, 624 (2003).
15. B.I. Abelev et al. (STAR Collaboration), nucl-ex/0801.3466
16. S. Voloshin and A.M. Poskanzer, Phy. Lett. **B414**, 27 (2000).